CHAPTER 1

INTRODUCTION

The human quest for flying higher and faster has made the world a global village and the desires to fly faster than the speed of sound has become a necessity now. Since the demonstration of the first sustained powered flight by Wright Brothers in 1903, the aerospace technology has grown leaps and bounds to achieve various milestones that have made our presence visible in the entire realm of the solar system. But the success story of human flight has carried a big baggage of failure. One such domain that has eluded the scientists and engineers is the conventional commercial supersonic flights. Although first manned supersonic flight was achieved in 1947, most of the supersonic flights to this date have been limited to military purposes only. The only commercial supersonic freighter Concorde was grounded and discontinued since 2003 following an accident that raised questions over human control of supersonic flight. The human flight story was pushed back decades with this event, with a present that is still void of civilian supersonic transport. Looking back into the aviation history, the initial successful flight attempts were made with flying machines which were monoplanes. A monoplane is a fixed planar wing with only one set of wing surface which can be a low wing, mid wing or a high wing configuration aircraft and the first monoplane was built-in 1874 by Felix de la Croix. In the late 1930s the monoplane with fixed wing was a common configuration for aircrafts. A typical monoplane configuration is shown in Fig. 1.1. A biplane is a set of two wing surfaces located one over other wherein both the wings provide a part of the total lift force. The lifts produced by both these wings are however, not the same. Generally, the lower wing is directly attached to the fuselage and the upper wing

is connected with to the fuselage with the struts and wires. The combinations of struts and wires provide the light and very strong structure. The biplane concept was first introduced by the Wright Brothers in 1903 through the successful flight of the Wright Flyer as can be seen in Fig. 1.2.

Fig. 1.1: monoplane configuration

Fig. 1.2: biplane configuration

Both the monoplane and the biplane configurations have their own advantages and disadvantages and preferred as per the mission requirements. The advantages and disadvantages of biplanes are listed below.

Advantages of biplane over monoplane:

- The biplane wings provide 20% more lift for the same wing area.

- The wing span for biplanes are less compared to monoplane, hence provides a better maneuverability.
- In biplanes struts and wires are used which provides a better strength to the wings.

Disadvantages of biplane over monoplane:

- There are two wings are used, hence the wings affect the aerodynamic properties of the others wing.
- The amount of drag produced by the biplane is more as compared to monoplane for higher speeds.
- For lower speeds biplane requires more surface area to provide the same lift.

1.1 **Supersonic Aircraft**

Supersonic aircraft are those, which has a speed more than that of the speed of sound. The supersonic flight is generally associated with the military fighter aircrafts and there are only a few civil supersonic aircraft in service now. Few of the popular supersonic transport aircraft that have successfully demonstrated the ability to overcome the sonic barrier are listed below along with their service periods.

	L/D	Service Period
Concorde	7.4	
SR-71	6.6	April 1962 to Dec. 1964
B-58	4.5	Nov. 1956 to Oct. 1965
XB-70	7.2	Sept. 1964 to Oct. 1965

The BELL XI was the first aircraft to fly at supersonic speed in 1947. Thereafter many military aircraft were designed to fly at supersonic speeds but the passenger supersonic aircrafts have not been so successful. The only supersonic jet with some success was the Concorde, shown in Fig. 1.3(a), but it operated only for a short route and was very expensive as well The Concorde could fly up-to a Mach

number of 2.04 with the payload of 92 to 128 passengers before retiring from the service due economic non viability. The first supersonic transport aircraft howevr was the Tupolev Tu-144, shown in Fig. 1.3(b), but it flew for a much less time than the Concorde due to the economical and safety issues [1].

(a) Concorde

(b) Tupolev Tu-144

Fig. 1.3: Supersonic transport aircrafts [1]

The fundamental problem with the supersonic commercial aircraft is the sonic booms. When an aircraft moves with supersonic speed, the shock waves are generated in front of the body and create sound like explosion called as the sonic boom. Sonic booms are unavoidable but can be minimized; the noise can be avoided by flying higher like the North American XB-70 which flew at 70,000ft as shown in Fig. 1.4, so that the frequency of sound near the ground can be

reduced. The Concorde flew over the surface of water to avoid the effect of the high intensity sonic boom on land. But this restricts the capabilities of supersonic commercial aircrafts. The need to redesign a supersonic transport aircraft with reduced intensity of sonic boom is paramount so as to make supersonic transport economically viable and less hazardous [1].

Fig.1.4: North American XB-70 Valkyrie [1]

Compared to military aircraft where cost is not important, the commercial aircraft have to overcome many challenges like *L/D* ratio increment, take-off and landing distances, efficient engine to provide high amount of thrust and the advance materials to resists the large shock loads, and vibrational loads etc. In addition to the above, the supersonic aircraft need to meet the environmental requirements. The supersonic commercial aircraft is successful only when it satisfies the both environmental requirements as well it is affordable to the users. The aerodynamic efficiency determined by the *L/D* ratio, is an extremely important parameter for supersonic aircrafts. The aerodynamic efficiency at supersonic speeds is highly influenced the wave drag which is excessive pressure drag caused by shock waves. As the speed of an aircraft increases from M_∞ = 0.8 to 1.2, the overall drag is increases rapidly i.e. approximately 4 times than drag at the subsonic speed. Because of this sudden increase in drag, the supersonic aircrafts need more engine power and stronger structure to withstand the stresses. The wave drag increments at supersonic speed can be reduced by making the fuselage section

longer, but this increases the overall weight of the aircraft and thus increases the overall power required.

The generation of lift in supersonic aircraft is also somewhat different from that in subsonic aircrafts. The L/D ratio for supersonic aircraft is generally half of the value for the subsonic aircraft, for example the L/D ratio for Concorde at cruise is 7.4, whereas for Boing 747 it is 17. Because of the low value of the L/D ratio in supersonic aircraft, additional thrust is required from the engines which have to run at lower efficiencies making it more difficult to meet the environmental requirements. The low L/D ratio also increases the design take-off weight, decreasing the range while increasing the fuel consumptions. [1]

1.2 Flow Behaviour at Supersonic Speeds

Supersonic aerodynamics deals with the flow problems wherein the speed of an object immersed in air is more than the speed of sound. Supersonic flow behaves very differently than the subsonic flows as in a supersonic flow the pressure disturbances emanating from an object cannot propagates upstream. In such a situation, fluid particles are not aware of the existence of the body downstream and it comes to know of the existence of the body only when it comes within its Mach cone. As a result the fluid particle cannot adjust itself to flow smoothly over the body as it would have done if the flow were subsonic and turns abruptly into itself just ahead of the object as shown in Fig. 1.5. The pressure disturbances thus, coalesce at a distance from the object to form a shock wave across which fluid properties changes drastically. The presence of shock wave is the main difference between the supersonic and subsonic flows and the prime sources of large drag and noise at supersonic speeds.

In supersonic flow the fluid particles experiences a sudden rise in pressure, density and temperature on crossing the shock wave. The flow velocity and the Mach number decrease across the shock wave. A detached bow shock is formed when the leading edge of the body is blunt or the free stream velocity is close to sonic velocity as shown in Fig. 1.5c [2].

Shock waves are not the only distinctive features of a supersonic flow. A quite contrasting phenomenon is a supersonic flow over an expansion corner wherein the flow is turned away from itself. In such a scenario, when a supersonic flow goes around a corner that turns away from the flow direction, then an expansion fan originates at the corner.

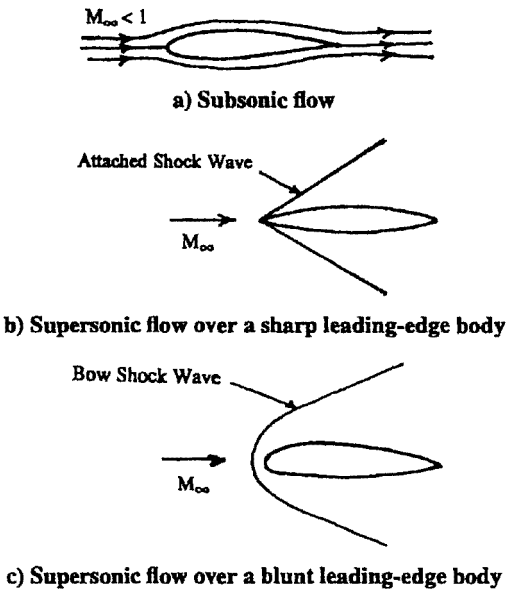

Fig. 1.5 High-speed flows over streamlined bodies [2]

In contrast to a shock wave, the temperature, pressure and density changes gradually across an expansion fan. On crossing an expansion wave, the pressure and temperature decreases and the free stream Mach number increases.

If the Mach number is in the high subsonic or low supersonic range, then the flow field around the body may consists of mixed subsonic and supersonic flow regions. When the Mach number is in the range of 0.8-1.2, the flow is said to be transonic. The evolution of complex flowfield from high subsonic Mach numbers to supersonic Mach numbers can be illustrated with the flow over an airfoil at a positive angle of attack as the freestream Mach number is gradually increased subsonic to transonic values. For a given freestream Mach number, there is a point on the top surface of the airfoil, like P where the local velocity is maximum

as given in Fig. 1.6a. At this point, the local velocity increases continuously as the freestream Mach number is increased. No drastic change in the nature of the flow takes place as long as the local flow everywhere on the airfoil is subsonic. When the Mach number reaches unity at point P, the free stream Mach number is called the critical Mach number and is denoted by M_{cr} as schematically illustrated in Fig. 1.6b. At other points on the surface of the airfoil, the Mach number is less than the unity and the flow is subsonic. The value of M_{cr} depends on angle of attack and the geometrical configuration of the body. For a given airfoil, the critical Mach number usually decreases with increase in α. The typical values of M_{cr} for airfoils at zero-lift lie in the range 0.6 – 0.85 [2].

As the Mach number increases beyond M_{cr}, the local velocity on the surface of the airfoil exceeds the sonic velocity at more than one point. In fact, a small region appears where the local Mach number is either equal to or greater than unity as shown in Fig. 1.6c. Because of fact that the flow Mach number behind the airfoil has to be equal to the freestream subsonic value, the region of supersonic flow is terminated by a normal shock wave as shown in Fig. 1.6c. As the freestream Mach number increases further but still below unity, the region of supersonic flow may even appear on the lower surface of the airfoil as shown in Fig. 1.6d. The formation of shock wave on the upper surface of the airfoil results in an adverse pressure gradient is impressed upon the boundary layer, causing it to separate from the surface. This separation of flow over the upper surface occurs well ahead of the shock wave. This is because of the fact that velocity near the body surface in the boundary layer is subsonic and therefore the formation of the adverse pressure gradient is communicated upstream of a shock wave through the boundary layer. The flow upstream of the shock wave is aware of the adverse pressure gradient and separate even before the shock wave, causing a modification in the effective body shape, hence a change in the shock wave structure.

As a result of the shock-induced flow separation, the drag coefficient rises very rapidly, and the lift coefficient drops as shown in Fig. 1.7 [2]. The drag coefficient

reaches a peak value around Mach 1 and then starts dropping off when a clear supersonic flow is established on the whole surface of the body.

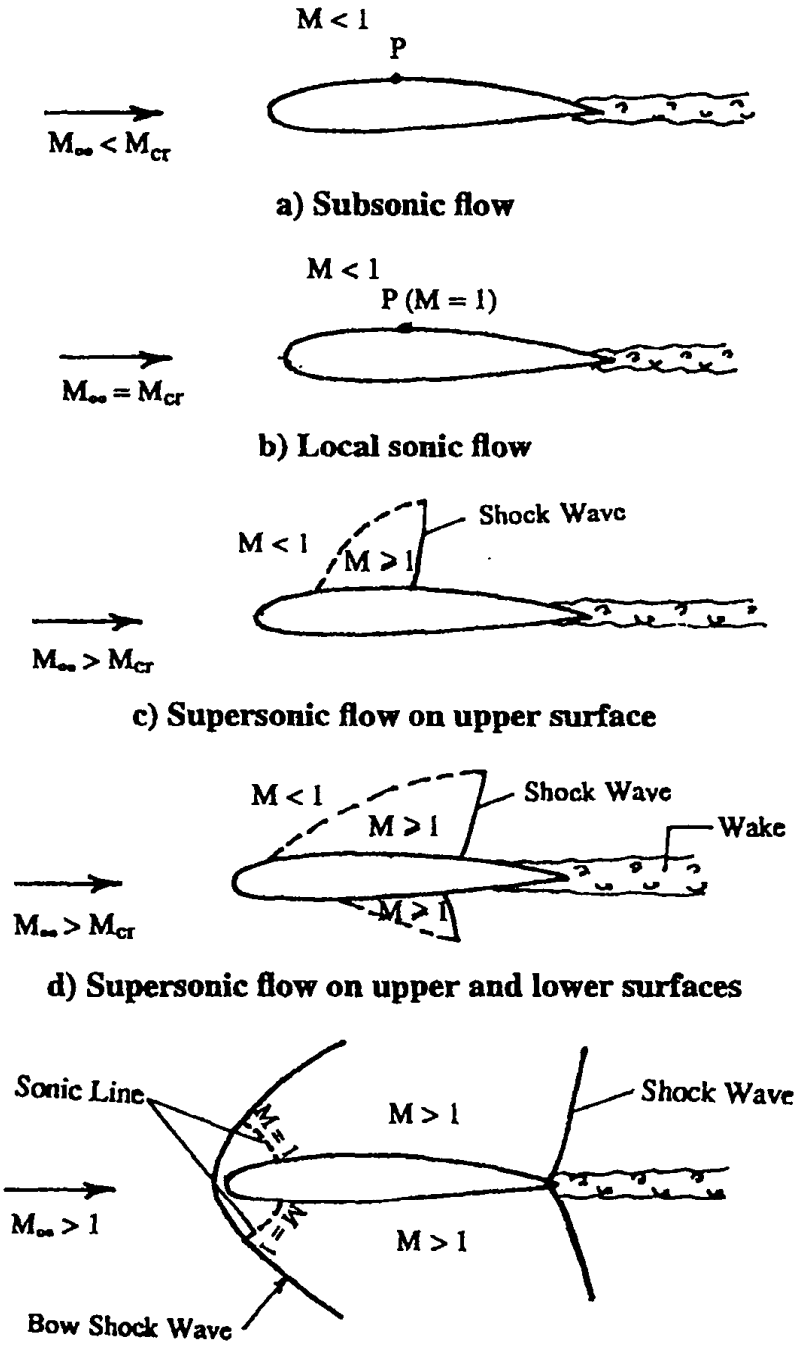

Fig. 1.6 Flow over airfoil at high speeds. [2]

When this happens, the flow separation point is pushed towards the trailing edge of the airfoil due to the formation of the shock waves on the lower as well as on the upper surface of the airfoil. The freestream Mach number at which the detrimental rise in drag is observed for a transonic flow over an airfoil is defined as the drag divergence Mach number.

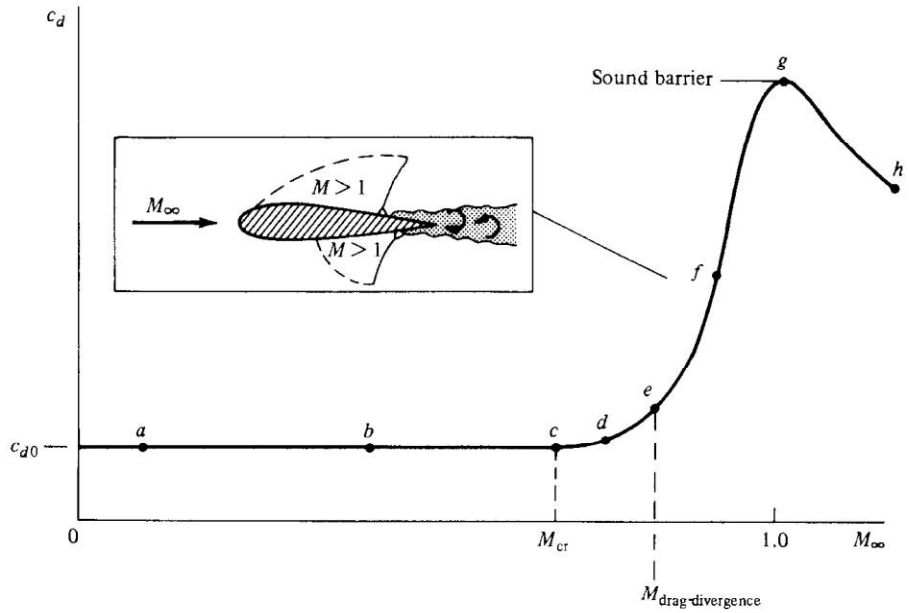

Fig. 1.7 C_D Variation with Mach number. [2]

The drag induced in high subsonic and transonic flow can be reduced by avoiding the detached shock wave by using a sharp edge airfoil. The shock wave is attached to the sharp corner of the airfoil and flow remains supersonic over the entire airfoil surface. One such airfoil used popularly at supersonic speeds is a diamond airfoil which is geometrically a sharp symmetrical double wedge at non lifting condition as shown in Fig 1.8.

Due to the sharp edge of the airfoil an oblique shock wave is formed at the leading edge, as a result, the pressure on surfaces AB and AD are higher than the freestream p_∞ because of the compression produced by the shock wave. At B and D, expansion fans are formed. The flow undergoes a gradual expansion and pressures on the surfaces BC and DC fall below the free stream value p_∞. Because pressure on AB and AD are equal, the net upward force or lift is zero. But the

axial components do not cancel, and we have a nonzero force in the axial direction. Similarly, the component of force in the direction normal to the flow on surfaces BC and DC cancel, but the axial components add up to give a nonzero force in the axial direction. The two nonzero axial force components add up to a net nonzero force in the flow direction, which is called wave drag. The wave drag is solely caused by the compressible nature of the fluid. Therefore, in supersonic flow, the wave drag is an additional component of the drag. Thus, for a given body, the drag in supersonic flow is usually much higher than that in subsonic flow. The wave drag depends on the geometrical shape and thickness ratio of the body and freestream Mach number. [2]

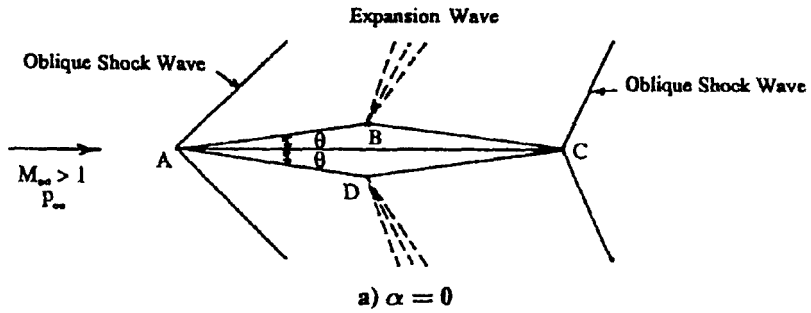

Fig. 1.8: Supersonic flow over double wedge airfoil at $\alpha = 0°$

At small positive angle α for the diamond airfoil, unequal strength shock waves were formed on the upper (shock wave AA') and lower surface (shock wave AA") of the diamond airfoil as shown in Fig. 1.9. The reason for this difference is that the flow turning angles for individual surfaces are not equal. Thus the pressure on AD is higher than that on AB. Similarly, the strengths of the expansion waves originating at B and D are different because Mach numbers on upper surface and lower surface are different. As the Mach number on the upper surface is generally greater than that on the lower surface, the pressure on BC is lower than that on DC. The net result is an upward force acting on the airfoil called as the lift force and a net force that along the free stream direction called the wave drag.

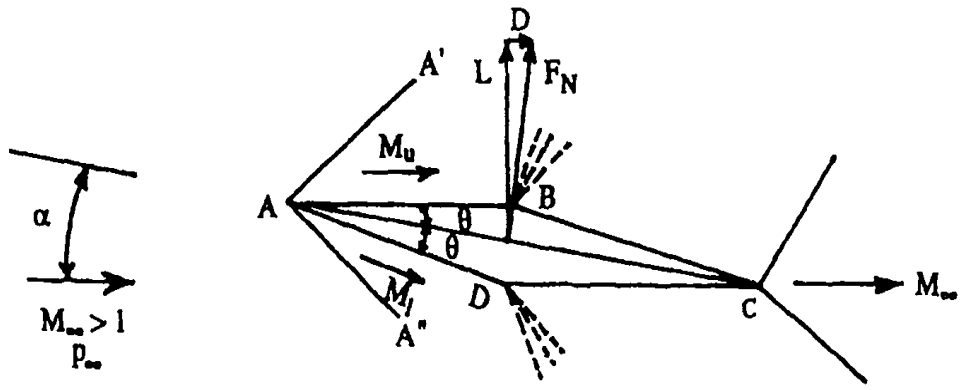

Fig. 1.9 Supersonic flow over double wedge airfoil at positive α. [2]

1.3 Shock Expansion theory

The quantification of lift and drag produced at supersonic speeds by any configuration, made up of straight edges can be done through the shock–expansion theory. The Shock expansion theory is a well-established classical theory for determining pressure forces on objects in supersonic flow regime. As the pressure forces dominate viscous forces at high speeds, it gives a fairly good estimate of the aerodynamic coefficients at supersonic speeds.

The understanding of the phenomena of formation of shock waves and expansion waves is a preamble to the estimation of aerodynamic forces though the shock expansion theory. If a slight disturbance takes place at some point in a gas, information is transmitted to other points in the gas through the sound waves and this disturbance propagates in all directions. The gas molecules which impact a disturbance body surface experience a change in momentum. In turn, this change is transmitted to neighboring molecules by random molecular collisions. In this fashion, information is propagated upstream of the surrounding at a speed of sound. If the upstream flow is subsonic the disturbances have no problem working their way far upstream, thus giving the incoming flow plenty of time to move out of the way of the body. However, if the flow is supersonic then the disturbances

cannot propagates upstream of the body, these disturbances coalesce in front of the body and creates a shock wave as shown in Fig. 1.10 (b).

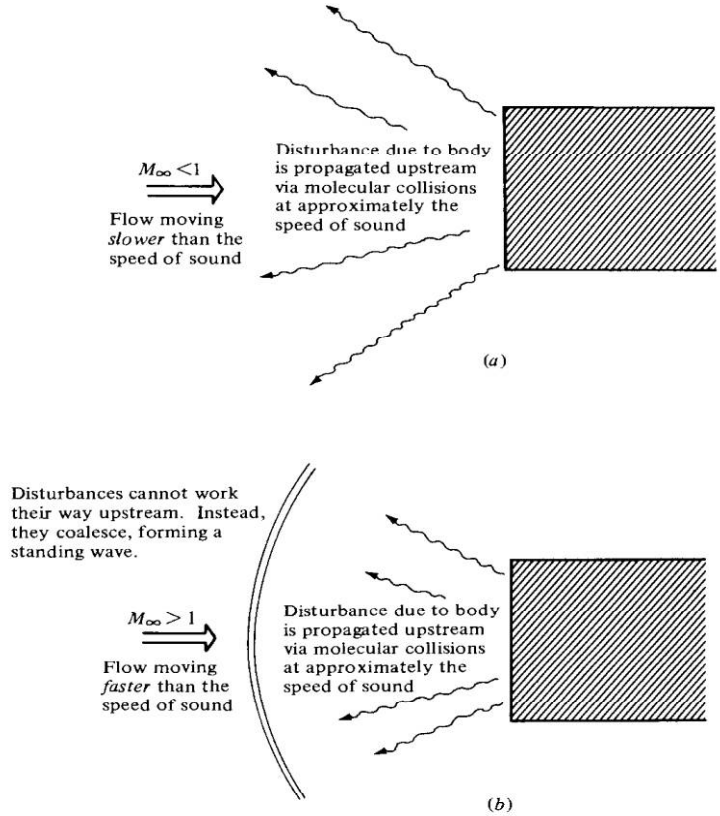

Fig. 1.10: Propagation of Disturbances. (a) Subsonic Flow. (b) Supersonic Flow. [3]

When the disturbing surface has a sharp leading edge the shock wave is attached to the leading edge and makes an oblique angle with respect to the freestream flow, and is called an oblique shock wave as shown in Fig. 1.11. In Fig. 1.11(a), the wall is turned upward at the corner through the deflection angle θ. In inviscid non-separated flows, the flow velocity is always tangential to the wall and thus the streamline at the wall is also deflected upward through the angle θ.

Whenever a supersonic flow is "turned into itself" as shown in Fig. 1.11(a), an oblique shock wave is formed. When the flow passes through the oblique shock wave the flow properties viz. pressure, temperature and density increase abruptly while the Mach number decreases. In contrast to this, when the wall is turned downward at the corner through the deflection angle θ, with the bulk of the gas is

above the wall, the streamlines are turned downward, away from the main bulk of the flow. In such cases, whenever a supersonic flow is "turned away from itself" as shown in Fig. 1.11(b), an expansion wave is formed. This expansion wave is in the shape of a fan centered at the corner. The fan continuously opens in the direction away from the corner. When the flow passes the expansion waves the flow properties viz. pressure, temperature and density decrease gradually while the flow Mach number increases [3].

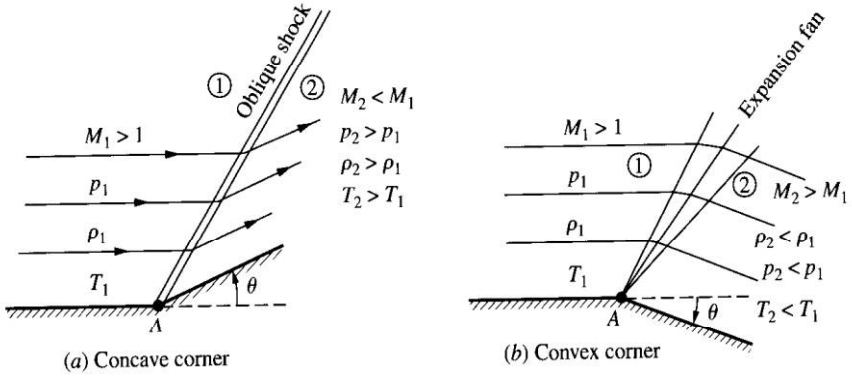

Fig. 1.11 Supersonic flow over a corner. [3]

The magnitude of change in flow parameters across an oblique shock wave needed for the shock expansion theory can be obtained by applying the conservation laws to a control volume having an oblique shock wave inside it as shown in Fig. 1.12. In Fig. 1.12, along with the control volume *abcdef*, a typical streamline is shown wherein the wave angle β is defined as the angle between the upstream flow direction and the shock wave. The upstream flow (region 1) is horizontal, with a velocity V_1 and Mach number M_1. In the downstream flow region (region 2) the flow velocity is V_2 and the Mach number M_2 is inclined at angle θ in upward direction. The velocity V_1 is split into components tangential and normal to the shock wave, w_1 and u_1, respectively, with the associated tangential and normal Mach numbers $M_{t,1}$ and $M_{n,1}$, respectively. Similarly, the downstream velocity is split into tangential and normal components w_2 and u_2, respectively, with associated Mach numbers $M_{t,2}$ and $M_{n,2}$, respectively. [3]

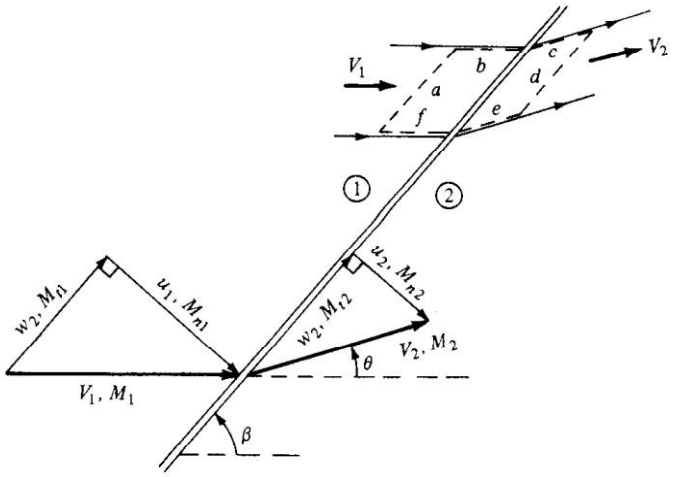

Fig. 1.12 Oblique shock geometry [3]

The application of the continuity equation to the control volume *abcdf* for a steady, inviscid, adiabatic flow with no body forces yield equation 1.1.

$$\oiint \rho V.dS = 0, \qquad \text{i.e. } \rho_1 u_1 = \rho_2 u_2 \tag{1.1}$$

The application of the law of conservation of linear momentum in a direction tangential to the shock wave gives the tangential component of momentum equation given by equation 1.2.

$$\oiint (\rho V.dS)w = -\oiint (PdS)_{tangential} \qquad i.e. \qquad w_1 = w_2 \tag{1.2}$$

Similarly, the application of the law of conservation of linear momentum in a direction normal to the shock wave gives the normal component of momentum equation given by equation 1.3.

$$\oiint (\rho V.dS)u = -\oiint (PdS)_{normal} \qquad i.e. \quad p_1 + \rho_1 u_1^2 = p_2 + \rho_2 u_2^2 \tag{1.3}$$

The first law of thermodynamics applied to control volume *abcdef*, gives the energy equation 1.4 for flow across an oblique shock wave.

$$\oiint \rho\left(e+\frac{V^2}{2}\right)V.dS = -\oiint pV.dS \qquad i.e. \qquad h_1+\frac{u_1^2}{2} = h_2+\frac{u_2^2}{2} \tag{1.4}$$

The governing equations 1.1, 1.2, 1.3 and 1.4 can be combined and with mathematical manipulation and assumptions of perfect gas and adiabatic flow can lead to relations for computation of post shock flow properties in terms of freestream Mach number M_1, shock wave angle β and the flow deflection angle θ. The shock wave angle β in itself is an unknown parameter and depends on the values of freestream Mach number M_1 and the flow deflection angle θ. The relation is thus an implicit one and given by equation 1.5.

$$tan\theta = 2cot\beta\frac{M_1^2sin^2\beta - 1}{M_1^2(\gamma + cos2\beta) + 2} \tag{1.5}$$

The above equation is often available as θ–β-M charts and for a given Mach number and flow deflection, the shock wave angle can be obtained. Once the shock wave angle is obtained the post shock properties can be computed using normal shock relations taking the normal component of the freestream Mach number and using the geometry in Fig. 1.12.

From Fig. 1.12 the component normal to the shock wave $M_{n,1}$ is given by equations 1.6.

$$M_{n,1} = M_1 sin\beta \tag{1.6}$$

Using the normal shock relations, the component of post shock Mach number normal to the oblique shock wave, $M_{n,1}$ can be computed using equation (1.7).

$$M_{n,2}^2 = \frac{1+[(\gamma-1)/2]M_{n,1}^2}{\gamma M_{n,1}^2 - (\gamma-1)/2} \tag{1.7}$$

Once the normal component of Mach number behind the shock wave is obtained, the downstream Mach number, M_2 can be determined from the geometry of the Fig. 1.12.

$$M_2 = \frac{M_{n,2}}{sin(\beta - \theta)} \tag{1.8}$$

Equation 1.5 provides two values of shock wave angle β, for a given freestream Mach number and flow deflection angle θ. For analytical computations, the lower value of β should be selected as the nature also prefers the weak solution for which post shock Mach numbers are supersonic in most cases. For a given freestream Mach number M_1, there is a maximum deflection angle θ_{max}. If the physical geometry is such that $\theta > \theta_{max}$, then there is no solution exists for a straight oblique shock wave. Instead nature established a curved shock wave, detached from the corner of the nose of a body as shown in Fig. 1.13. In such a scenario the analytical computations cannot be obtained and solutions are obtained through the numerical means using iterative solvers.

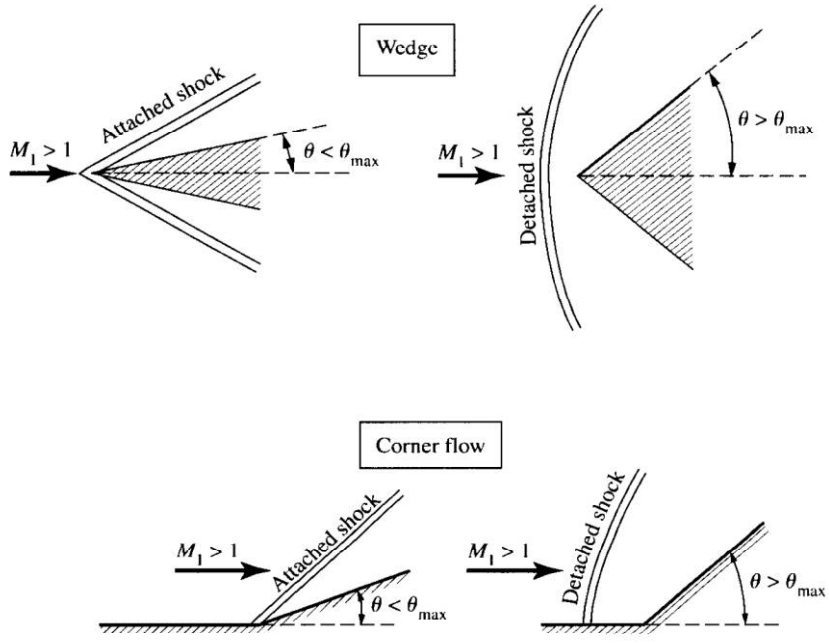

Fig. 1.13 Attached and detached shock [3]

The lift in supersonic flows is generally obtained because of flow expansion on upper surface of wing. These expansions occur through an expansion fan which is formed when a supersonic flow is "turned away from itself" as shown in Fig. 1.14. The expansion fan is a continuous expansion region that can be visualized as an infinite number of Mach waves, each making the Mach angle μ with the local flow direction.

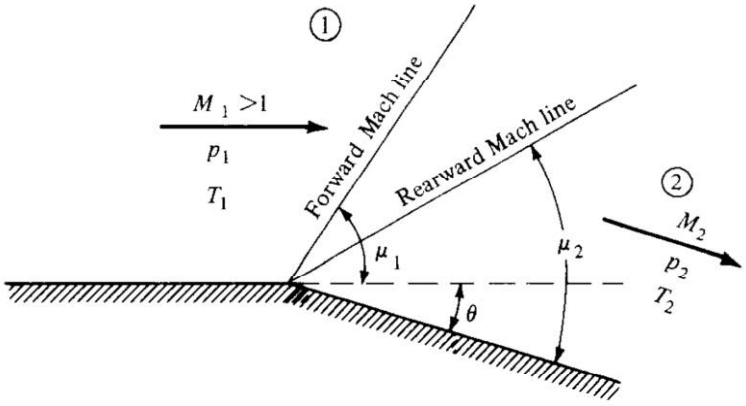

Fig. 1.14: Expansion Wave

The expansion fan is bounded upstream and downstream by the Mach waves which make the angle μ_1 and μ_2 with respect to the upstream flow. An expansion fan is an isentropic phenomena and the differential change in the flow direction at a given Mach number across is related to the corresponding differential change in velocity by equation 1.9.

$$d\theta = \sqrt{M^2 - 1}\frac{dV}{V} \tag{1.9}$$

Equation 1.9 can be integrated from region 1, where the deflection angle is zero and the Mach number is M_1, to region 2, where the deflection angle is θ and the Mach number is M_2 as shown in Fig. 1.14. This results in equation 1.10

$$\theta = \nu(M_2) - \nu(M_1) \tag{1.10}$$

In equation 1.10, ν is called the Prandtl-Meyer function, an explicit function of the freestream Mach number and is given by equation 1.11

$$\nu(M) = \sqrt{\frac{\gamma+1}{\gamma-1}}\tan^{-1}\sqrt{\frac{\gamma-1}{\gamma+1}\left(M^2-1\right)} - \tan^{-1}\sqrt{M^2-1} \qquad (1.11)$$

Once the Mach number in the region is established using equations 1.10 and 1.11, the properties in the post expansion fan region can be computed with the knowledge of isentropic relations. The use of *θ-β-M* charts and the Prandtl-Mayer function helps establish the value of pressure and velocity magnitude in different distinct regions of flow over an airfoil. Two typical examples of how the shock wave theory and the expansion wave theory can be utilized to compute the aerodynamic forces on bodies in inviscid supersonic flows are shown in Figs. 1.15 and 1.16.

Fig. 1.15 shows supersonic flow over a flat plate of chord length c is placed at an angle of attack α. Because of the flow turning away on the upper surface, there is an expansion wave on the upper surface starting at the leading edge the flat plate. Due to this the magnitude of pressure p_2 is less than the freestream pressure p_1. On the lower surface the magnitude of the pressure p_3 is more than the upstream pressure, due to the shock wave is generated on lower side of the flat plate. At the trailing edge of the flat plate the flow must be parallel to the free stream direction, hence a shock wave on the upper surface and an expansion wave on the lower surface are generated and makes the flow direction parallel to the free stream.
The top and the bottom surfaces of the flat plate experiences uniform pressure distribution of p_2 and p_3 wherein p_3 is greater than p_2. This creates a net pressure imbalance that generates the resultant aerodynamic force per unit span *R*', whose magnitude is given by equation 1.12

$$R' = (p_3 - p_2)c \qquad (1.12)$$

The components of forces in parallel and perpendicular directions to the freestream are then evaluated as given by equations 1.13 and 1.14.

$$L' = (p_3 - p_2)c\cos\alpha \qquad (1.13)$$

$$D' = (p_3 - p_2)c\ sin\alpha \tag{1.14}$$

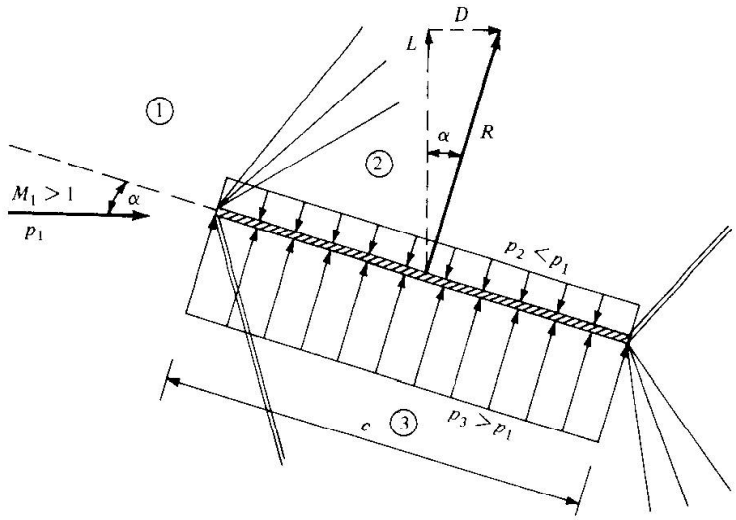

Fig. 1.15: Supersonic flow over a flat plate at positive α.

The flowfield around a diamond-shaped airfoil at α = 0° in a supersonic flow is shown in Fig. 1.16. At the leading edge the flow is turned by and angle ε and the compression takes place through oblique shock waves on the top and the bottom surface. Due to the compression effect the pressure on the surfaces 'a' and 'c' is more than the freestream pressure. At the mid-point of the diamond airfoil the flow is expanded at the upper and lower points through continuous expansion waves by an expansion angle 2ε and the pressure are decreases. The magnitude of the pressures on the surfaces 'b' and 'd' are identical but lower than the pressures at 'a' and 'c'. At the trailing edge of the airfoil the flow direction is again changed and flow becomes parallel to the freestream direction through oblique shock waves. The magnitude of the pressures on top and bottom surfaces of the diamond airfoil at zero incidence is symmetrical and hence the overall lift of the diamond airfoil is zero. But the magnitude of pressures in the drag direction is more for the surfaces 'a' and 'c', therefore the finite drag is produced by the diamond airfoil.

The magnitude of the drag force per unit span can be calculated from the airfoil geometry using equation 1.15.

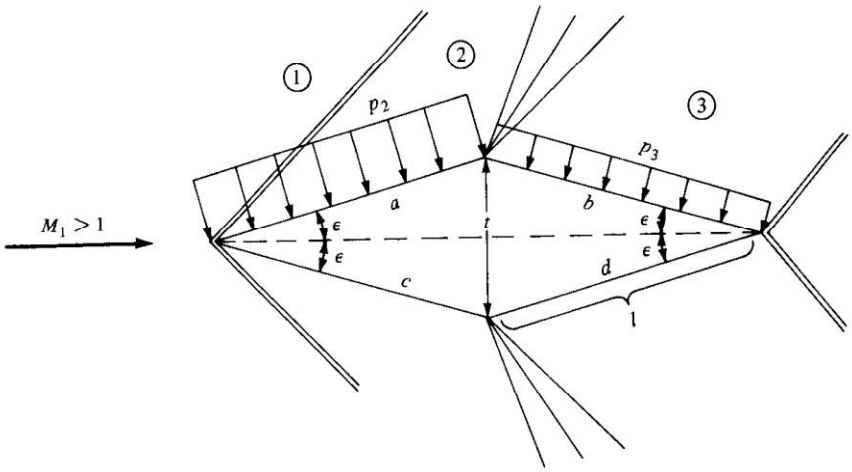

Fig. 1.16: Diamond airfoil in a supersonic flow at $\alpha = 0^{o}$. [3]

$$D' = 2(p_2 l \sin\varepsilon - p_3 l \sin\varepsilon) = (p_2 - p_3)t \qquad (1.15)$$

In equation 1.15, t is half the maximum thickness of the airfoil and l is the length of the each face of the airfoil. In Equation 1.15, the magnitude of pressure p_2 is calculated from oblique shock theory, and p_3 is calculated from the expansion theory. Moreover, these pressures are the exact values for supersonic, inviscid flow over the diamond airfoil.

The supersonic flows illustrated in Figs. 1.16 and 1.17 are the simplest of examples and the real life supersonic flows can be quite complex. The presence of multiple surfaces in an actual flying object creates multiple oblique shocks which interact with one other to produce a complex flowfield which is difficult to analyze analytically and numerical solutions are often required to decode the flowfield under such situations. Nevertheless for simple cases of shock wave interactions wherein two shock waves of either same or opposite families intersect, the flowfield aft of the interaction can be obtained through pressure deflection analysis and heat and trial methods. There are many kinds of sock-shock interactions in a complex flowfield; some of them have analytical solutions as explained below.

1.4 Shock Interactions and Reflections

In real life situations, the oblique shock impinges somewhere on another solid surface and/or intersects other waves, either shock or expansion waves. Such wave interaction is important for the designing of supersonic aircraft. A typical shock interaction and reflection consider a supersonic flow past a concave corner is shown in Fig. 1.17. In Fig. 1.17 the angle of the corner is θ and β_1 is the wave angles at the concave corner and a straight horizontal wall is present above the concave corner. The shock wave induced from the concave corner A, called the incident shock, impinges on the horizontal wall at point B and is reflected after the interaction at point B and called as the reflected shock wave thereafter. The flow direction is inclined upward at angle θ due to the concave corner in the region 2 as given in Fig. 1.18. The direction of the flow must be tangential to the wall in region 3 due to the presence of the horizontal wall.

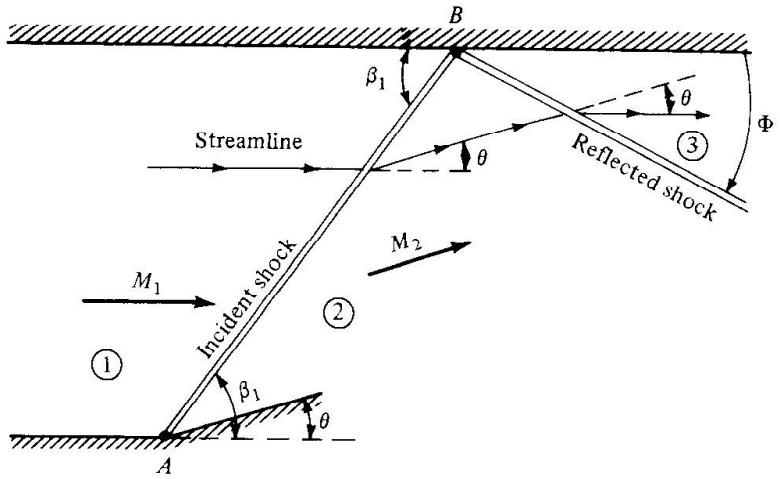

Fig. 1.17: Regular reflection of a shock wave from a solid boundary. [3]

Hence the flow direction in region 2 must be bend trough the same angle in order to maintain a flow tangential to the upper wall; hence a second shock wave called the reflected shock wave is induced at point B. The main purpose of this shock is to maintain a flow, in region 3, parallel to the upper wall. The Mach number M_2 in

region 2 is greater than M_1, the Mach umber in region 1. Thus the strength of the reflected shock is less as compared to the incident shock although the deflection angles for both the shocks is the same, therefore the reflected shock angle ϕ is also lower than the incident shock angle β_1.

Another type of shock-shock interaction that is common in those between the shock waves of opposite families as shown in Fig. 1.18. Here, the shock waves A and B generated by the concave corners at point G and H, propagate downwards and interact at point E to change their directions and give distinctive flowfields in regions 4 and 4'.

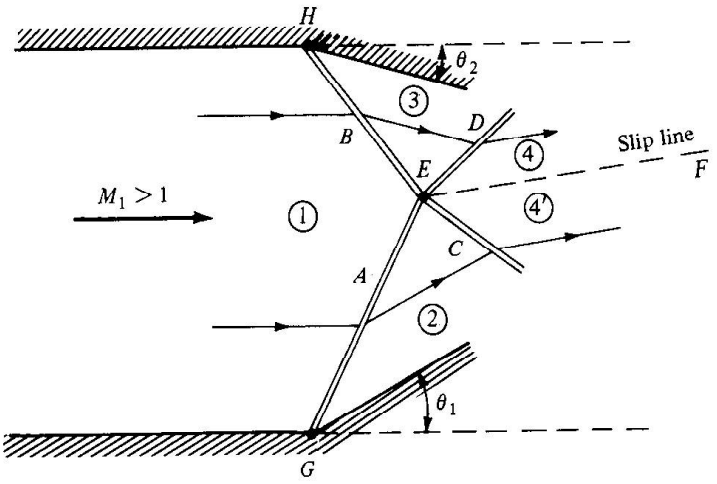

Fig. 1.18: Intersection of shock waves

At the interaction point E, the shock wave A is refracted and generates a refracted shock wave D in the upward direction at point the interaction and a flow aft of it denoted by 4. Similarly the shock wave B refracted at point E and generates a shock wave C downstream of the interaction point E and the flow region aft of the refracted wave is denoted by 4'. The flow properties in the regions 4 and 4' are different due to the different wave angle and the different strength of the shock waves after the interaction at point E. These two regions are divided by the line EF, called the slip line, the pressure and the direction of the flow across the slip

line remains same while the entropy and velocities are different. The flowfields in these regions can be estimated using heat and trial methods or numerically.

Another complex phenomenon in supersonic flows that is difficult to analyze analytically is the interaction of the shock waves with the viscous boundary layers. Most of the formulations discussed in the previous sections have the assumptions of inviscid supersonic flows wherein the governing equations are hyperbolic in nature and slightly easier to analyze. In real situations the interactions between the shock waves and the viscous boundary layers can be quite complex as explained below.

1.5 Shock wave-boundary layer interactions

Shock waves and boundary layers do not mix; bad things can happen when a shock wave impinges on a boundary layer. Unfortunately, shock-wave/boundary layer interactions frequently occur in practical supersonic flows. A typical shock wave boundary layer interaction is represented by an oblique shock wave impinging on a boundary layer as shown in Fig. 1.19 wherein we can see a boundary layer growing along a flat plate. Although the external flow is supersonic, the boundary layer velocity profile is subsonic near the wall. In Fig. 1.19 at some downstream location an incident shock impinges on the boundary layer. The large pressure rise across the shock wave acts as a severe adverse pressure gradient imposed on the boundary layer, thus causing boundary layer to locally separate from the surface. Because of the high pressure behind the shock feeds upstream through the subsonic portion of the boundary layer, the separation take place ahead of the theoretical inviscid flow impingement point of the incident shock wave. In turn, the separated boundary layer deflects the external supersonic flow into itself, thus inducing a second shock wave, identified here as the induced separated shock wave. The separated boundary layer subsequently turns back towards the plate, reattaching to the surface at some downstream location. Here again the supersonic flow is turn into itself, causing a third shock wave called the reattachment shock. Between the separation and reattachment shocks, where the

boundary layer turns back towards the surface, the supersonic flow is turned away from itself, generating expansion waves as shown in Fig. 1.19.

At the point of reattachment, the boundary layer becomes relatively thin, the pressure increases considerably, and consequently this becomes a region of high local aerodynamic heating. Further away from the plate, the separation and reattachment shocks merge to form the conventional reflected shock wave that is expected from the inviscid flow.

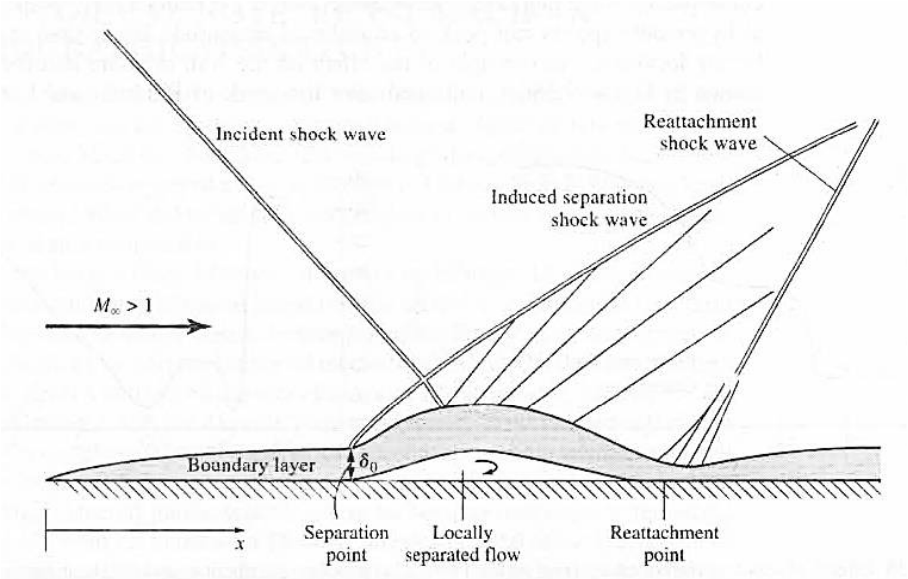

Fig. 1.19: Shock-wave Boundary Layer Interarction

The scale and the severity of the interaction shown in Fig. 1.19 depend on whether the boundary layer is laminar or turbulent. Since laminar boundary layers separate more readily than turbulent boundary layers, the laminar interaction usually takes place more readily with more severe attendant consequences than the turbulent interactions. However, the general quality aspects of the interaction shown in Fig. 1.18 are the same for both cases. [3]

There is a large attendant increase in drag for configurations in compressible flow regime especially at the supersonic Mach numbers. These flows are complicated more so by the presence of complex phenomena like the shock wave-boundary

layer interactions and the shock-shock interactions. Nevertheless many techniques and theories have established themselves as means to overcome the problems of compressibility and reducing the subsequent pressure drag evident in highly compressible flow regimes including supersonic ones. Few of the popular methods are discussed below.

Thin Airfoil: The thinner the airfoil, the smaller is the peak local velocity on its surface and higher is the critical Mach number as shown in Fig. 1.20.

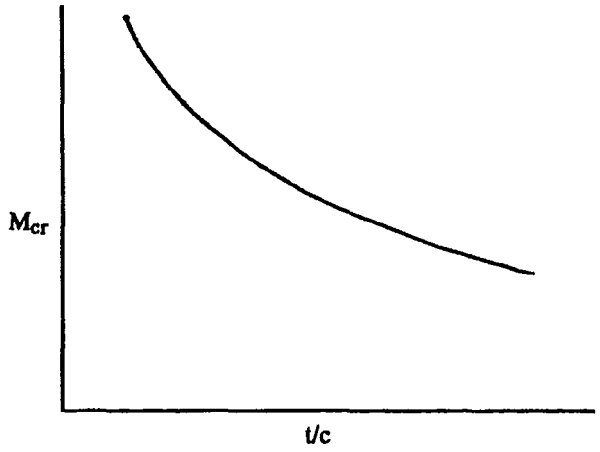

Fig. 1.20: Variation of Critical Mach number with thickness/chord ratio [2]

The use of thin airfoils pushes the critical Mach number, M_{cr} and the drag divergence Mach number, M_{dd} further towards unity. However, a disadvantage of using very thin airfoil is that their low-speed characteristics, especially the stalling characteristics are poor. The sudden loss of lift at stall for thin airfoils can lead to stability problems [2].

Low-aspect ratio wings: The lower the aspect ratio of a wing, the more pronounced are the induced flow effects and lower are the peak velocities on the wing surface. As a result, the critical Mach number increases with a decrease in aspect ratio as shown schematically in Fig. 1.21 [2].

Supercritical airfoils: For a conventional airfoil at Mach numbers above the critical Mach numbers, the local region of supersonic flow terminates in a strong shock wave that induces significant flow separation and a steep rise in the drag coefficient. For supercritical airfoil shown in Fig. 1.22, the curvature of the middle region of the upper surface is substantially reduced with a resultant decrease in strength and extent the shock wave. As a result, the drag associated with the shock wave is reduced and, more importantly, the onset of separation is substantially delayed. The lift lost by reducing upper surface curvature is regained by substantial camber of the rear portion of the supercritical airfoil.

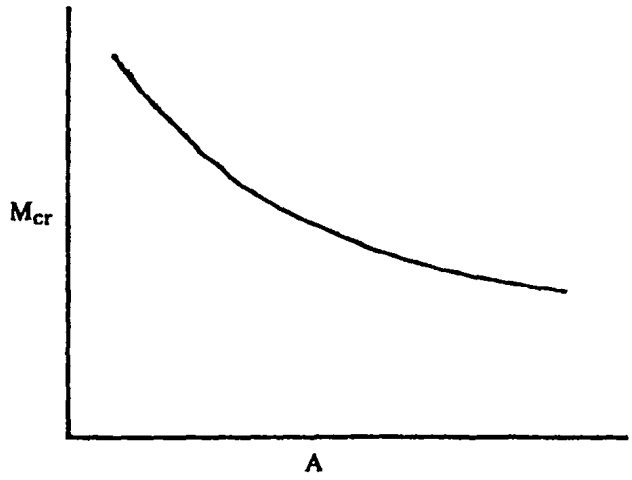

Fig. 1.21 Variation of critical Mach number with aspect ratio [2]

Wing sweep: The concept of wing sweep is a powerful method of delaying the adverse effects of compressibility and pushing the critical Mach number to much higher values and even beyond Mach 1. On the surface of the wing the velocity component normal to the wing leading edge i.e. $V_\infty cos\Lambda$ affects the pressure distribution. The spanwise component $V_\infty sin\Lambda$ does not alter the pressure distribution and therefore, the free stream Mach number at which the critical condition occurs on the wing is increased by a factor of $1/ V_\infty cos\Lambda$ compared to a straight, unswept wing as shown in Fig. 1.23. The critical Mach number for the

swept wing is $M_{cr}/V_{\infty}cos\Lambda$ for a sweep angle of Λ, where M_{cr} is the critical Mach number for the straight wing.

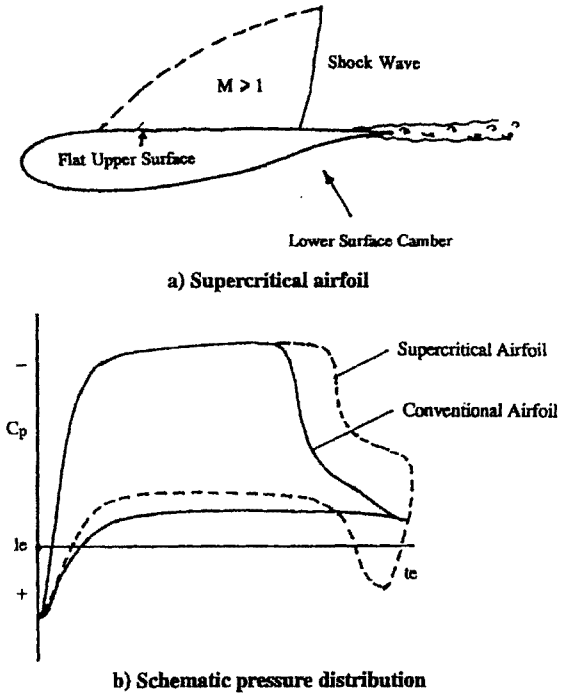

Fig. 1.22 Schematic illustration of flow over supercritical airfoil [2]

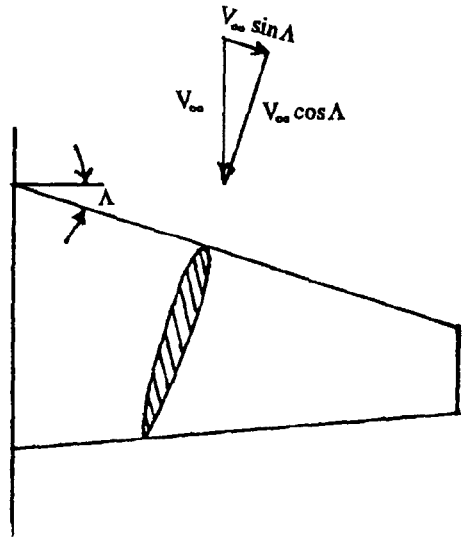

Fig. 1.23: Schematic illustration of effect of wing sweep [2]

Delta wing: The delta wings have their leading edges swept behind the Mach cone and this provides an efficient method of reducing the wave drag. However, at low speeds the increased sweep causes difficulty in maintaining attached flow even at moderate angle of attack. Flow separation occurs at quite modest values of angles of attack and tends to spread in an unpredictable way. This often causes serious stability and control problems. The most troublesome of these are the separations that originate at the leading edge and rolls up into a vortex sheet. The point of origin of these leading edge separations were difficult to tie down because the swept back wing had a round leading edge. This had led aerodynamicists to believe that the requirements for high and low speed flights are in direct conflict. [2]

The emergence of thin slender, sharp-edged delta wing has solved this problem. The flow over a sharp edge delta wing differs significantly from that over a sweepback with round leading edge. The most important difference is that the flow separation occurs right at the sharp leading edge and, in this way, flow separation points are fixed for all angles of attack. With fixed flow separation points, the problems associated with unpredictable stall progression of the swept back wings is eliminated. Along with this, many of the stability and control problems associated with the uncertainty in flow separation pattern of the swept back wing also disappears.

On delta wing the separated flow on the leeside rolls up to form a spiral over the wing as shown in Fig. 1.24. The pressure in the vortex core is considerably lower as shown in Fig. 1.24(b) and as a result a substantial lift increment is obtained. This incremental lift is called vortex lift and is associated with the large mass of air accelerated downward by the vortex sheet. This solves the problem of lift deficiency associated with swept-back wings. Thus with delta wings, a new concept of controlled flow separation came into existence that represented a departure from the time-honored concept of attached flow [2].

Under this new concept, a wing is designed for attached flow at supersonic cruise condition and at low speeds; the flow is allowed to separate at the leading edge and generate the beneficial vortex lift.

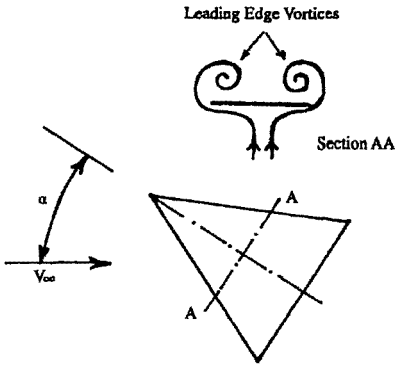

a) Delta wing at angle of attack

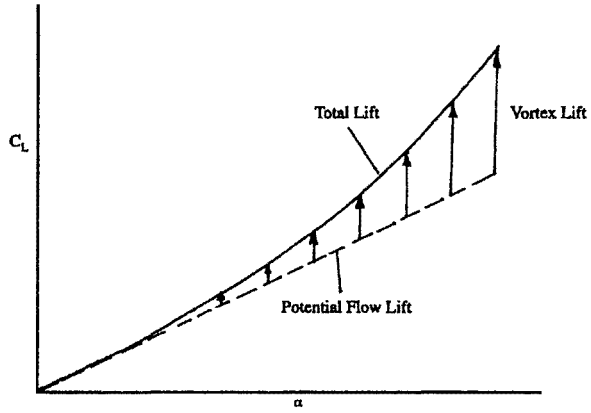

b) Variation of lift coefficient with angle of attack

Fig. 1.24: Delta wing in low-speed flow at angle of attack [2]

Oblique wings: If we need good low-speed characteristics combined with good high speed characteristics such as low wave drag, then we have to use a variable sweep wing. However, one of the main disadvantages of the variable sweep wing is the large weight penalty associated with the additional structure required to handle structural loads. With Oblique wings, a straight wing is rotated in flight, such that at low speeds it is essentially at zero sweep angles and at high speeds, one wing is swept forward and the other is sweep back as shown in Fig. 1.25.

An oblique wing is continuous from tip to tip and is attached to the fuselage at only one point called as the pivot. The bending moment on one half of the wing is neutralized by the other half and as a result, the pivot carries only the lift load; hence the wing structure is much lighter [2].

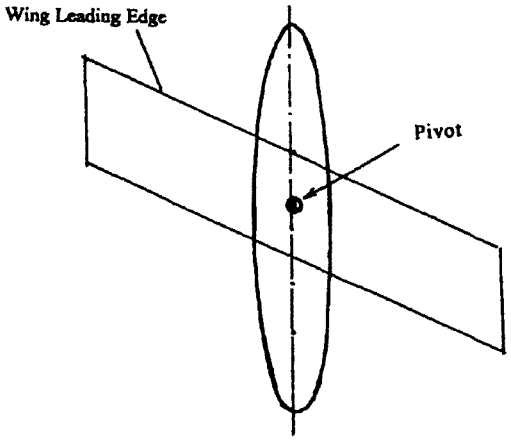

Fig. 1.25: An oblique wing [2]

Another significant advantage of the oblique wing is the absence of aerodynamic center shift at transonic speeds. On a conventional variable geometry wing at transonic speeds, the aerodynamic center moves aft as the wing sweep increases to reduce the wave drag. This creates more nose-down moment and requires a large horizontal tail surface to trim the aircraft. This increases the trim drag and hence affects the performance of the aircraft. With the oblique wing, this problem is considerably alleviated as one half of the wing sweeps aft and the other half id swept forward and the overall aerodynamic center hardly moves. Therefore, a large horizontal tail is not needed to trim the aircraft in transonic speeds.

1.6 Wave Elimination: biplane concept

Using thin airfoil theory for 2-D supersonic airfoils, for the small α, the lift and wave drag coefficients of a flat plate can be given by equations 1.16 and 1.17.

$$C_L = \frac{4\alpha}{\sqrt{M_\infty^2 - 1}} \tag{1.16}$$

$$C_D = \frac{4\alpha^2}{\sqrt{M_\infty^2 - 1}} = \frac{\sqrt{M_\infty^2 - 1}}{4} C_L^2 \tag{1.17}$$

For n parallel plates at an angle of attack α, the lift coefficient produced by the combination is same as the single flat plate as shown in Fig. 1.26. Assuming the chord of the flat plate is the same in both cases and the angle of attacks α and α_s are related as

$$\alpha = \frac{\alpha_s}{n} \tag{1.18}$$

where α_s is the angle of attack for a single flat plat. For the same lift coefficient the wave drag for the combination can be given by equations 1.19[4].

$$D = n \frac{4}{\sqrt{M_\infty^2 - 1}} \left[\frac{\alpha_s}{n}\right]^2 qc = \frac{1}{n}\left(\frac{4}{\sqrt{M_\infty^2 - 1}} \alpha_s^2\right) qc \tag{1.19}$$

It is clear from the above expression that for same lifting conditions, the wave drag produced by the n parallel plate is *1/n* times then the wave drag produced by a single flat plate, whereas the skin friction drag for the combination is increased by n times because of increment in the surface area of the n parallel plates. [4]

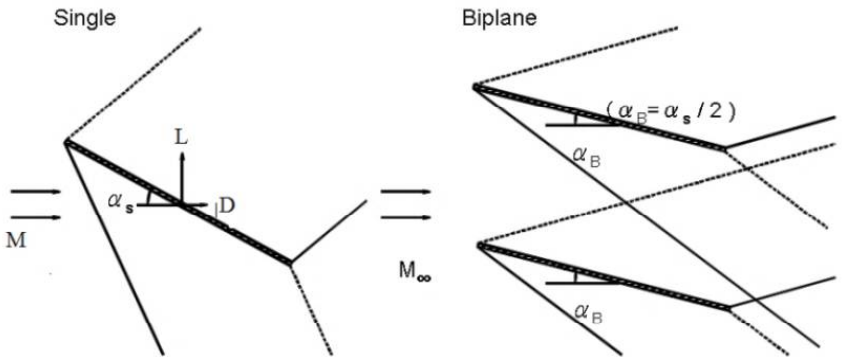

Fig. 1.26: Wave reduction effect [4]

For multiple airfoil configurations, the overall lift produced by the individual elements is reduced and hence the drag produced by the individual element is also reduced. For the entire configuration the lift remains same but it is redistributed. This effect is called the wave reduction effect as suggested by Kusunose [4].

1.7 Wave cancellation effect

The wave drag due to the airfoil thickness is also reduced by the biplane configurations. By choosing appropriate locations of the biplanes in the geometry of the configuration, the wave drag can be eliminated by the wave cancellation effect. At zero lift condition Busemann biplane shows a complete elimination of the wave drag for the combination at M_∞ = 1.7.The Busemann biplane configurations is formed by simply placing the inverted half diamond airfoil one above the other as shown in Fig. 1.27 such that the geometrical dimensions are $t/c = 0.1$, $z = 0.5$c and wedge angle $\varepsilon = 5.71°$.

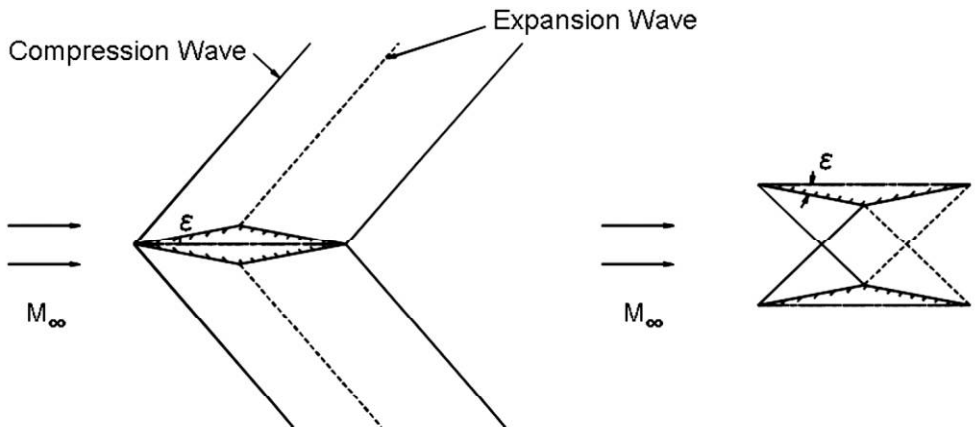

Fig. 1.27: Wave cancellation effect of the Busemann airfoil [4]

At M_∞ = 1.7, the strong shock formed at the leading edge of the configuration, strikes at the point of maximum thickness of the other element and interact with the expansion waves and thereby cancelling effect of shock and expansion waves and theoretically eliminating the wave drag is completely [4]. But at off-design conditions of $M_\infty > 1$, the shock wave angle is smaller and hence the shock waves do not impinge at the point where the expansion wave starts as shown in Fig. 1.28

(b), hence the wave drag is increased, but due to the shock interaction between the elements, the value the wave drag is less than the simple diamond airfoil.

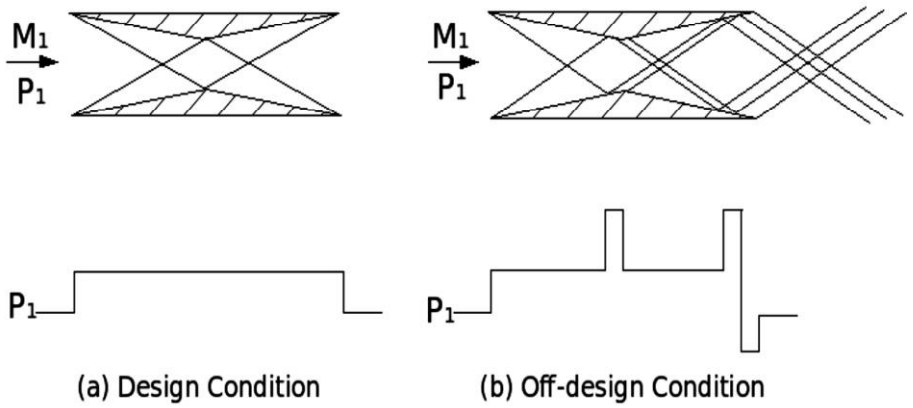

Fig: 1.28: Shock structure and pressure distribution for Busemann Biplane.

1.8 Start/Un-start condition of Busemann biplane

Although the biplane configuration is very useful at design Mach number, there is a need to discover the methods that can be improve the off-design condition of the Busemann biplane. Also flow between the Busemann biplanes is similar to that of a convergent divergent inlet diffuser as the two elements are very close and the flow interactions between these elements are similar to internal supersonic flows. As with the internal flow between a convergent divergent diffuser, the supersonic flow between the biplanes also have to overcome the starting problem. Below the starting Mach numbers, the flow between the biplanes is choked due to the formation of a normal shock wave that increases the wave drag of the configurations with subsonic flow between the planes. As with the convergent divergent diffusers, for a given ratio of throat area to the inlet area, the Mach number required to start the system is given by the Kantrowitz limit [5]. Once the detached shock is generated in front of the biplanes or for the inlets, the freestream Mach number must exceed the starting Mach number so as to start the diffuser from the unstart condition. This starting Mach number for a given throat

to inlet area as shown in Fig. 1.29 is given by the Kantrowitz limit and can be evaluated through Eq. 1.20[5].

$$\frac{A_t}{A_i} = \left[\frac{(\gamma-1)M_\infty^2+2}{(\gamma+1)M_\infty^2}\right]^{1/2}\left[\frac{2\gamma M_\infty^2-(\gamma-1)}{\gamma+1}\right]^{-1/(\gamma-1)} \tag{1.20}$$

where A_t is the area of throat and A_i is the area of the inlet.

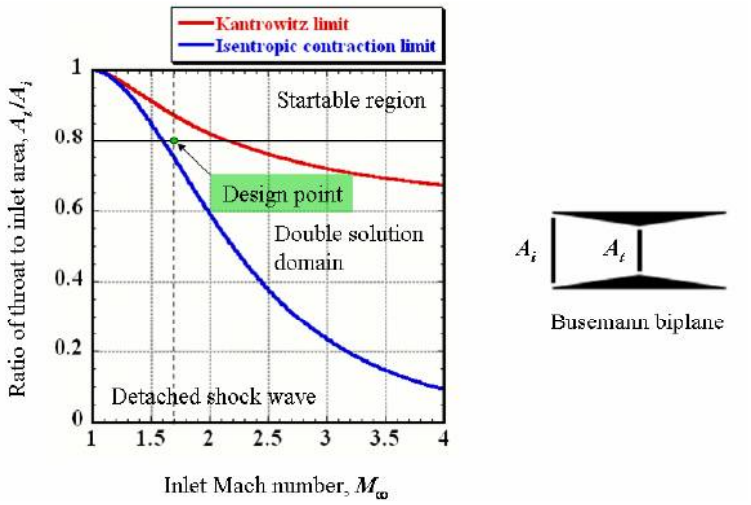

Fig. 1.29: Starting Mach Number for Supersonic Inlets [5]

1.9 Supersonic Airfoil Development

Airfoil is the most critical component of an aircraft on which the lifting capability of aircraft is dependent. According to the Lynch about 2/3 of the total drag of an aircraft is produced by the wing itself, hence it is very important to choose the correct shape of the wing so as to produce a minimum amount of drag [6].

The scientific airfoil development began in early 19th century. A significant milestone was achieved in1884 when H F Philips tested a series of airfoil design for extremely low Reynold's Numbers. Afterwards many scientists tested different airfoil series by trial and error for the specific requirements, but Eastman Jacob at NACA in 1939 developed the first laminar flow airfoil section for

making an airplane fly faster as compared to other series. These airfoils were thinner and symmetrical in section and the leading edges were more pointed [6]. Even after more than a decade of the research in airfoil developments, there is no generic method or rule for airfoil development as every design of airfoils is specified according the uses and to the flow conditions under which it operates. For supersonic flights, wing with low value of wave drag and the low intensity of the sonic boom are preferred. A strong detached bow shock wave generated in front of a blunt wing at supersonic speeds produces a large amount of pressure drag. Hence supersonic airfoils have a sharp leading edge so that an attached oblique shock wave is formed which much weaker than a bow shock wave and hence the high pressure zone ahead of the leading edge is eliminated to give a reduced wave drag. Other the side the sharp leading edge airfoil has very high stalling speed and requires very large runways in subsonic flights. In 1960's the idea is using shock wave cancellation effect in supersonic aircraft was introduced. The Shaped Sonic Boom Demonstration (SSBD) program successfully demonstrated the reduction in the intensity of sonic boom by aircraft shaping [7]. Recently Kusunose proposed a new generation supersonic transport aircraft design as shown in Fig. 1.30.

Fig. 1.30: Conceptual Boomless Supersonic Transport Aircraft [5]

His research group has carried out both computational fluid dynamics (CFD) and wind tunnel experiments [5, 8, 9, 10 and 11] to establish the use of supersonic

biplanes. They first studied the advantages and disadvantages of the Busemann biplane configuration in supersonic flow and designed a two dimensional Busemann type biplane airfoils at non-lifting and lifting conditions. Furthermore, they have proposed a modified biplane using inverse designed method. Kusunose et al. have proposed the concept of leading edge and trailing flaps for improvement of the poor performance of the Busemann biplane at off-design conditions.

As the requirement to fly faster is growing in today's rapidly changing global scenario, there is a need to design and develop a next generation supersonic transport aircraft that can satisfy the economy requirements of low sonic boom and reduced the wave drag for sustainable development.

Organization of the Thesis

The current chapter has highlighted the various aspects of supersonic flow and introduced the concepts supersonic biplanes along with the problems associated with such configurations.

In Chapter 2, a literature review of past work is done so as to explore the state of the art on the aerodynamics of supersonic biplanes and its derivatives with improved performance. Chapter 3 provides the motivation behind choosing the current subject for research and also highlights the key objectives of the research based on the literature review in Chapter 2. In Chapter 4 the numerical tools that forms the CFD methodology used in this investigation is explained in detail. This includes the physical, mathematical and numerical model of the fluid dynamic problem under investigation along with the pertinent numerical procedure. Chapter 5 presents detailed numerical results for the work carried out in the research. This includes discussion on the flowfield structure around staggered biplanes with sharp and rounded leading edges at various Mach numbers and angles of attack. Finally, in Chapter 6 the main outcomes of the current research are outlined along with recommendations for future work directions.